Original Research Article

Assessment of Topsoil Geotechnical Competency and Overburden Protective Capacity Using Geoelectrical Methods in Gwarinpa, Abuja

ABSTRACT

This study presents an integrated geophysical and geotechnical assessment of the subsurface in the Gwarinpa area, aiming to characterize soil competency and aquifer vulnerability to guide sustainable urban development. The investigation, employing electrical resistivity techniques and geotechnical analysis, reveals a subsurface dominated by a weathered basement complex with shallow, unconfined aquifers. Findings indicate that the sandy topsoil offers good drainage but exhibits low unconfined compressive strength (55-78 kPa), rendering it incompetent for supporting heavy structures without stabilization. Furthermore, the aquifer protective capacity is rated as moderate to poor across most of the area, with critically vulnerable zones identified in the western and eastern sectors where the overburden is thin and fractured. Based on these results, the study concludes that soil stabilization is imperative for any significant construction. It provides critical recommendations for urban planning, including the use of generated zoning maps to direct infrastructure away from vulnerable areas, the enforcement of land-use regulations to protect groundwater, and the necessity for site-specific geotechnical investigations. This research underscores the efficacy of combining geophysical and geotechnical methods to de-risk urban development and ensure long-term environmental and structural integrity.

Keywords: Geotechnical Characterization; Aquifer Vulnerability; Electrical Resistivity; Soil Competency; Urban Geophysics; Subsurface Mapping

1.0 INTRODUCTION

Engineering structures are designed and constructed for maximum durability. Beyond the loss of financial investment, structural failure can lead to severe consequences, including loss of life and property. All structures rely on foundations, the design of which is critically dependent on the characteristics of both the structure and the underlying soil or rock. Consequently, the nature of the supporting soil is paramount for ensuring safety, structural integrity, and the longevity of the superstructure. Determining soil strength is thus vital for evaluating the competence and stability of earth materials, providing crucial data on their ability to withstand stresses from loads and environmental factors. Conventionally, civil engineers have preferred direct methods like the Cone Penetration Test (CPT) and other geotechnical investigations to assess subsoil strength for supporting infrastructure (Rajapakse, 2016).

Beyond structural integrity, the subsurface also plays a critical role in environmental protection, specifically in shielding underlying aquifers from surface-borne contaminants. The same overburden layers that provide foundational support also act as a natural filter, with their thickness and clay content determining the groundwater's vulnerability to pollution. Key factors contributing to both foundation failure and aquifer contamination often share a common root: inadequate subsurface characterization. This can lead to poor foundation design on incompetent soils and the siting of potential contaminants like septic tanks in areas with thin, permeable overburden.

These factors, in combination, can lead to catastrophic structural damage. Therefore, there is a pressing need to accurately estimate and characterize soil properties for sound engineering planning and management (Ofomola et al.,2018). While laboratory testing of soil samples is a conventional approach, it is often point-specific and costly. However, significant resistivity contrasts often exist between the conductive overburden and the resistive basement bedrock, allowing geophysical methods to effectively delineate subsurface layers and depth to bedrock (Akintorinwa and Abiola, 2011). Geophysical surveys, particularly 1D Vertical Electrical Sounding (VES), provide spatially extensive information on soil resistivity, layer thickness and lithology, which has been successfully correlated with subsoil competence (Idornigie & Olorunfemi, 2006) and with the protective capacity of the overburden.

Recent geophysical investigations across Nigeria have consistently demonstrated the efficacy of electrical resistivity in conducting integrated subsurface assessments. Studies in diverse geological settings, including Abuja (Alaminiokuma and Chaanda, 2019; Samuel et al., 2022; Agada & Yakubu, 2022), southwestern Nigeria (Adeyemo et al., 2022; Bayowa et al., 2023; Olatunji-Adeniyi et al., 2024), southeastern Nigeria (Azuoko et al., 2023) and in the Middlebelt of Nigeria (Ayua et al., 2024, 2025), have successfully utilized geoelectrical parameters to simultaneously evaluate geotechnical competency for foundations and aquifer vulnerability to contamination. This established methodology reliably delineates zones of risk, confirming the critical role of such integrated approaches in guiding sustainable urban development and environmental protection.

This study aims to assess a dual assessment of geotechnical competency of the topsoil and evaluate the protective capacity of the overburden materials in the basement complex terrain of Gwarinpa, Abuja, using geoelectrical methods. The frequent incidence of building failures in Nigeria can be attributed not only to poor construction materials but also to incompetent subsurface geomaterials. Furthermore, the siting of potential contaminants like septic tanks and dumpsites without considering the overburden's protective capacity poses a significant risk of aquifer contamination. This research leverages the cost-effective and rapid VES technique to provide vital information on layer resistivity, thickness, and lithology, enabling a comprehensive evaluation of overburden protective capacity and the categorization of the area into zones of varying geotechnical competence. Consequently, there is an urgent need for thorough geophysical and geotechnical investigations to ascertain the bearing capacity and strength of foundation materials to ensure sustainable and safe safe construction practices and protect critical groundwater resources, thereby supporting resilient urban development.

1.1. LOCATION AND GEOLOGY OF THE STUDY AREA

The study area, Gwarinpa, is located within the Federal Capital Territory (FCT), Abuja, approximately between **longitude** $7^{O}23^{I}$**53.**74^{O}**E and latitude** $9^{O}4^{I}2.34N$.. The FCT is situated north of the confluence of the Niger and Benue rivers and is bounded by Niger State to the west and northwest, Kaduna State to the northeast, Nassarawa State to the east and south, and Kogi State to the southwest. Gwarinpa is a well-developed district in Abuja's Phase 3, renowned for the expansive Gwarinpa Housing Estate. The area boasts good road networks and substantial residential and commercial development.

Geologically, Abuja lies within the Nigerian Basement Complex, predominantly composed of Precambrian metamorphic and igneous rocks which cover about 85% of the territory, with the remaining 15% consisting of Cretaceous sedimentary rocks from the Bida Basin (Akoachere et al., 2019; Etuk et al., 2022). The tectonic fabric of the area, characterized by N–S to NNE–SSW trending structures, is a legacy of the Pan-African Orogeny, which involved the collision of the West African craton with the Pan-African mobile belts (Alagbe, 1979).

2.0 MATERIALS AND METHODS

2.1. DATA ACQUISITION AND PROCESSING

This study utilized the Vertical Electrical Sounding (VES) technique. A total of forty (40) VES stations were established across the study area (Fig. 1) using the Schlumberger electrode array. This array was chosen for its depth penetration efficiency. The half-current electrode separation (AB/2) was progressively increased from 0.5 m to 150 m, while the potential electrode spacing (MN/2) varied from 1 m to 5 m. An ABEM SAC300C Digital Resistivity Meter was employed, powered by a 12V battery source with a transmitted current of 1 milli-ampere. The apparent resistivity was calculated and recorded for each electrode configuration. The fundamental apparent resistivity (ρa) for the Schlumberger array is given by:

$$\rho_{a(s)} = \pi R \frac{\left(\frac{AB}{2}\right)^2}{MN} \quad (1)$$

The calculated apparent resistivity (ρa) values were plotted against AB/2 on bi-logarithmic graph paper to derive preliminary layer models. This was achieved by means of partial curve matching techniques described in Eze and Ayua (2025). To enhance objectivity and accuracy, these initial models were subsequently refined using Winresist 1D inversion software (Vander Velpen, 2004), which provides a best-fit model and quantifies parameter uncertainty. Maximum iterations for the forward modelling was pre-set to 30 and the resulting output with an RMS error of less than 5% was accepted for the study (Joshua, *et. al.* 2023). The end product of this computer assisted forward modeling were the primary geoelectric parameters of layer resistivity and thickness.

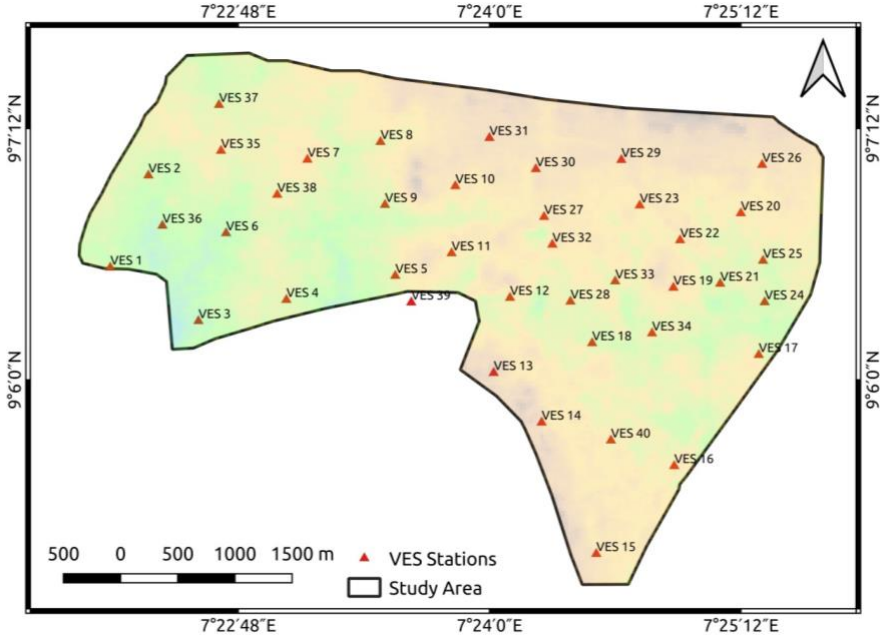

Figure 1: VES station distribution in the Study Area.

2.2 DERIVATION OF SECONDARY GEOELECTRIC PARAMETERS

From the primary parameters of layer resistivity (ρi) and thickness (hi), several secondary geoelectric parameters were computed after Ayua (2025) to aid in the analysis of aquifer vulnerability and soil character. These included:

(a) Longitudinal unit Conductance S = $\sum_{i=1}^{n} \frac{h_i}{\rho_i}$ (2)

(b) Transverse unit Resistance T = $\sum_{i=1}^{n} h_i \rho_i$ (3)

(c) Longitudinal Resistivity = $\rho_i = \frac{h_i}{S_i}$ (4)

(d) Transverse Resistivity = $\rho_t = \frac{T_i}{h_i}$ (5)

The dependence of resistivity on the direction of current flow is known as electrical anisotropy (Olorunfemi *et al.,* 1991). The Electrical coefficient of anisotropy in the entire column may be computed from these directional resistivities (ρ_l and ρ_t) and the Dar-Zarrouk parameters (S and T) as:

Electrical Coefficient of Anisotropy (λ) = $\sqrt{\frac{\rho_t}{\rho_l}} = \sqrt{\frac{\sum h_i \tilde{n}_i \sum \frac{h_i}{\rho_i}}{(\sum h_i)^2}}$ (6)

In an isotropic medium, $\rho_1 = \rho_2$ (vertical resistivity); hence, $\rho_t = \rho_l$. It implies that $\lambda = 1$.

2.3. ASSESSMENT OF SOIL COMPETENCY

Geophysical techniques, particularly electrical resistivity, have proven invaluable for rapid assessment of subsoil competency. A well-established correlation exists between soil resistivity and lithology, with clayey materials (low resistivity) generally exhibiting lower bearing capacity. The soil competency classification scheme developed by Idornigie and Olorunfemi (2006), as shown in Table 1, was adopted for this study. This rating was applied to the topsoil resistivity map to generate a geotechnical competency zonation map for the study area.

Table 1: Soil Competency Rating Based on Apparent Resistivity *(after Idornigie and Olorunfemi, 2006)*

Apparent Resistivity (Ω·m)	Inferred Lithology	Competence Rating
< 100	Clay	Incompetent
100 – 350	Sandy clay	Moderately competent
350 – 750	Clayey sand	Competent
> 750	Sand / Laterite / Bedrock	Highly competent

2.4 Determining Overburden Protective Capacity

The protective capacity of the aquifer overburden was evaluated using an integrated analysis of key geoelectrical parameters derived from Vertical Electrical Sounding (VES) data.

2.4.1 Overburden Thickness

The overburden thickness, defined as the cumulative thickness of all unsaturated strata overlying the aquifer unit, was determined for each VES location. This thickness (H) is calculated as:

$$H = h_1 + h_2 + \ldots + h_n \quad (7)$$

where h_1 to h_n represent the thicknesses of individual layers constituting the aquifer overburden. Greater overburden thickness generally provides enhanced physical attenuation and longer contaminant travel times, contributing to higher protective capacity.

2.4.2 Integrated Electrical Conductivity (IEC)

The Integrated Electrical Conductivity, expressed as Longitudinal Conductance (S), serves as a direct indicator of the clay content within the overburden sequence. Since clay-rich layers act as natural hydraulic barriers due to their low permeability, the longitudinal conductance provides a quantitative measure of the overburden's ability to retard contaminant migration (Ayua et al., 2024). The calculated values were classified according to established protective capacity ratings:

Table 2: Longitudinal conductance/aquifer protective capacity rating (Oladapo et al., 2004)

Longitudinal conductance (mhos)	Aquifer protective capacity rating
>10	Excellent
5 – 10	Very Good

0.7 – 4.49	Good
0.2 – 0.69	Moderate
0.1 – 0.19	Weak
< 0.1	Poor

2.4.3 Electrical Coefficient of Anisotropy

The Coefficient of Electrical Anisotropy (λ) was computed to assess subsurface heterogeneity and potential preferential flow paths. It is derived from the Dar-Zarrouk parameters using the equation:

$$\lambda = \frac{\sqrt{TS}}{H} \quad (9)$$

where H represents total overburden thickness, S denotes longitudinal conductance, and T indicates transverse resistance. Higher anisotropy values (λ >> 1) suggest the presence of fractures, joints, or structural discontinuities that act as secondary porosities (Ayua, 2025) and can compromise protective capacity by creating rapid pathways for contaminant transport.

2.4.4 Composite Protective Capacity Analysis

A weighted overlay analysis integrating the Electrical Coefficient of Anisotropy, Integrated Electrical Conductivity, and Overburden Thickness was performed with equal weighting among parameters. The normalized composite values were classified using the natural breaks method to generate a comprehensive aquifer protective capacity map, delineating zones of varying vulnerability across the study area.

2.4. LABORATORY SOIL TESTING

Six (6) disturbed soil samples were collected from shallow pits (0.2-0.3 m depth) at selected locations within the study area. The samples were subjected to standard laboratory tests to determine their geotechnical properties. These tests included: moisture content (by oven drying), grain size distribution (by sieve analysis and hydrometer), Atterberg Limits (for Plasticity Index, PI), standard Proctor compaction (ASTM D698), and unconfined compressive strength (UCS, ASTM D2166). It is crucial to note that the compressive strength results, originally reported in kN/m³, are corrected and discussed in the standard unit of kilopascals (kPa) in Section 3.4.

3.0 RESULTS AND DISCUSSION

3.1. VERTICAL ELECTRICAL SOUNDING (VES) INTERPRETATION

The interpreted VES data revealed a subsurface comprising 3 to 5 geoelectric layers. The curve types encountered included 3-layer (H, A), 4-layer (HA, HK, QH), and 5-layer (HKH, HKA) curves. The H-type curve was the most predominant, constituting 27.5% of the soundings. Other significant curve types were KH (20.0%), HA (17.5%), QH (10.0%), and HKH (10.0%). According to Worthington (1977), VES curve types reflect the underlying lithologic sequence. The dominance of H-type and related curves signifies a weathered basement environment, where groundwater occurrence is primarily within the weathered layer, and the aquifers are mostly unconfined.

The topsoil resistivity and thickness values ranged from 19.7 to 389 Ω-m and 0.5 to 2.18 m respectively. The wide range of topsoil resistivity values is indicative of variable layer composition consisting of unsaturated clay / sandy clay / clayey sand / sand / laterite. The weathered layer resistivity and thickness values ranged from 4.3 to 877 Ω-m and 3.8 to 44.7 m respectively. The weathered layer constituted the main aquifer unit in the study area. The fresh basement resistivity values ranged from 105.2 to 8,794 Ω-m. About 45% of the entire study area had fresh basement resistivity above 1000 Ω-m. The study area is located within basement complex geology. The aquifer zones in the basement complex areas are predominantly made up of the

Weathered/fractured basement complex rocks. The main aquifer identified from the study area was the weathered and or fractured basement, with very minimal occurrence of fractured aquifers present as revealed from the VES interpretation. The aquifers tend to be localized and vary greatly in thickness ranging from 3.8 to 44.7 m with only a few fractured/confined basement aquifers encountered within the study area. The overlying weathered and or topsoil rocks represented the confining structure on the underlying aquifers where the lithology permitted, otherwise, a majority of the aquifer within the study area are unconfined.

3.2. TOPSOIL COMPETENCY ZONATION

The spatial distribution of topsoil resistivity, presented as an iso-resistivity map (Fig. 2), shows the topsoil resistivity and thickness values ranged from 19.7 to 389 Ω-m and 0.5 to 2.18 m (Fig. 3) respectively with an average resistivity of about 120 Ω-m. The wide range of topsoil resistivity values is indicative of variable layer composition consisting of unsaturated clay / sandy clay / clayey sand / sand / laterite. Pockets of low resistivity (indicative of clayey materials) are distributed along the margins of the study area, while zones of higher resistivity (>300 Ω-m) are found in the southwest and southeast.

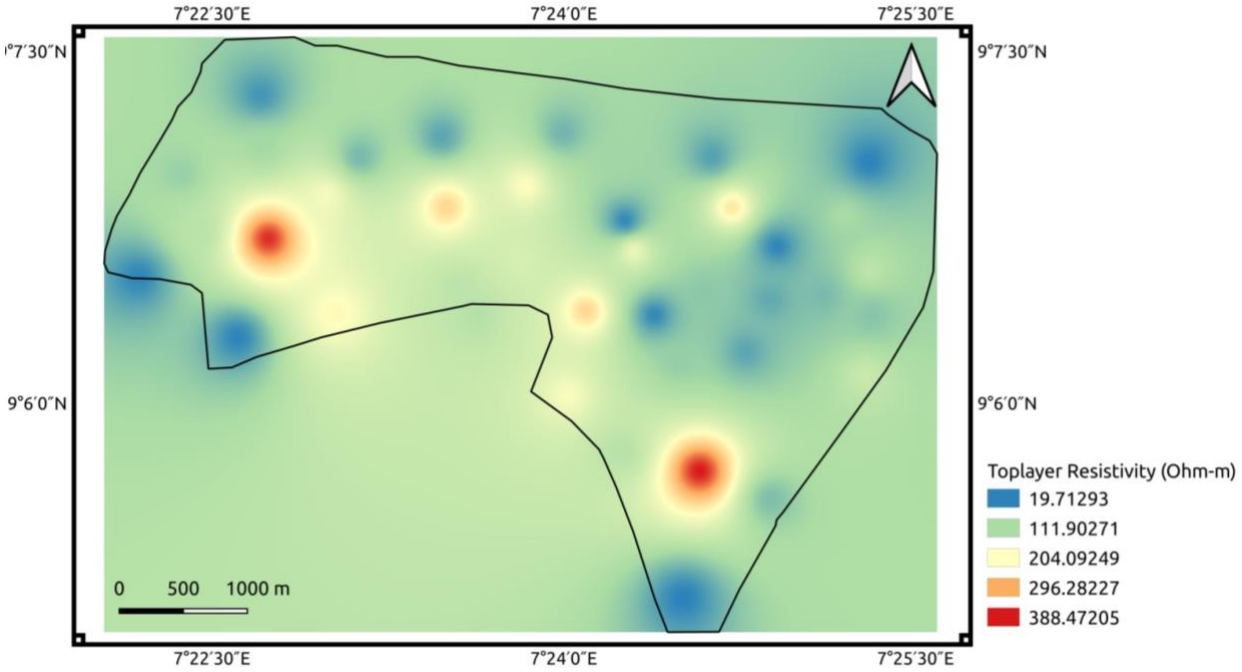

Figure 2: **Isoresistivity map of the topsoil**

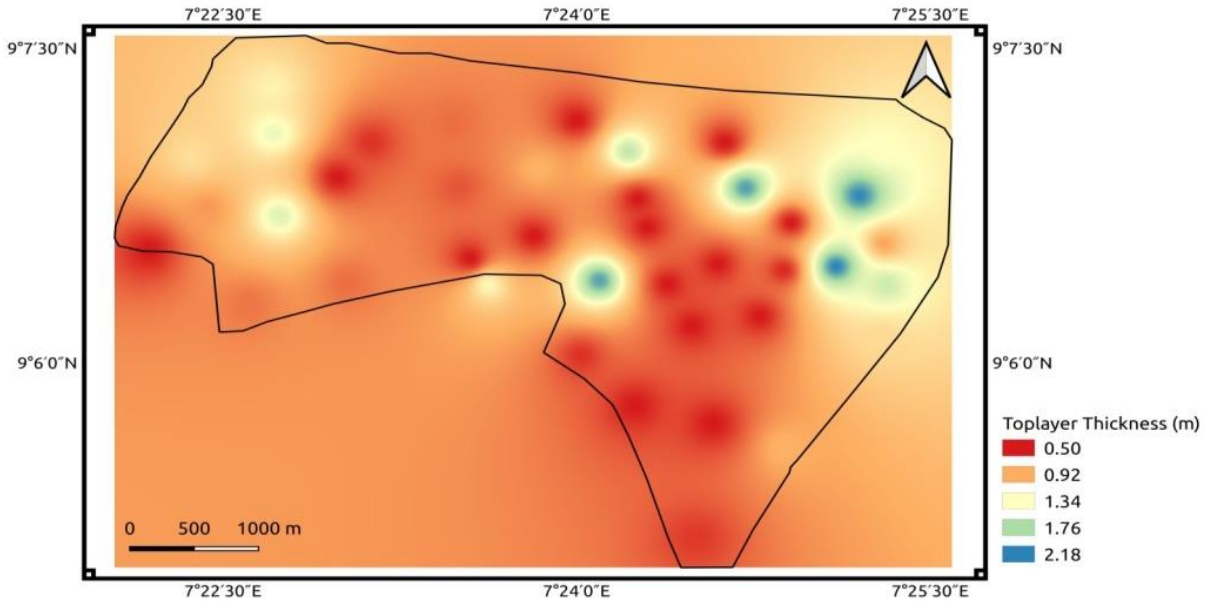

Figure 3: Toplayer thickness distribution map of the topsoil

Using the classification in Table 1, the study area was zoned into competence categories presented on Figure 4. The largest portion of the area is classified as **Moderately Competent** (sandy clay lithology). Approximately 35% of the area is **Incompetent** (clay), and two isolated zones are classified as **Competent** (likely clayey sand or shallow laterite).

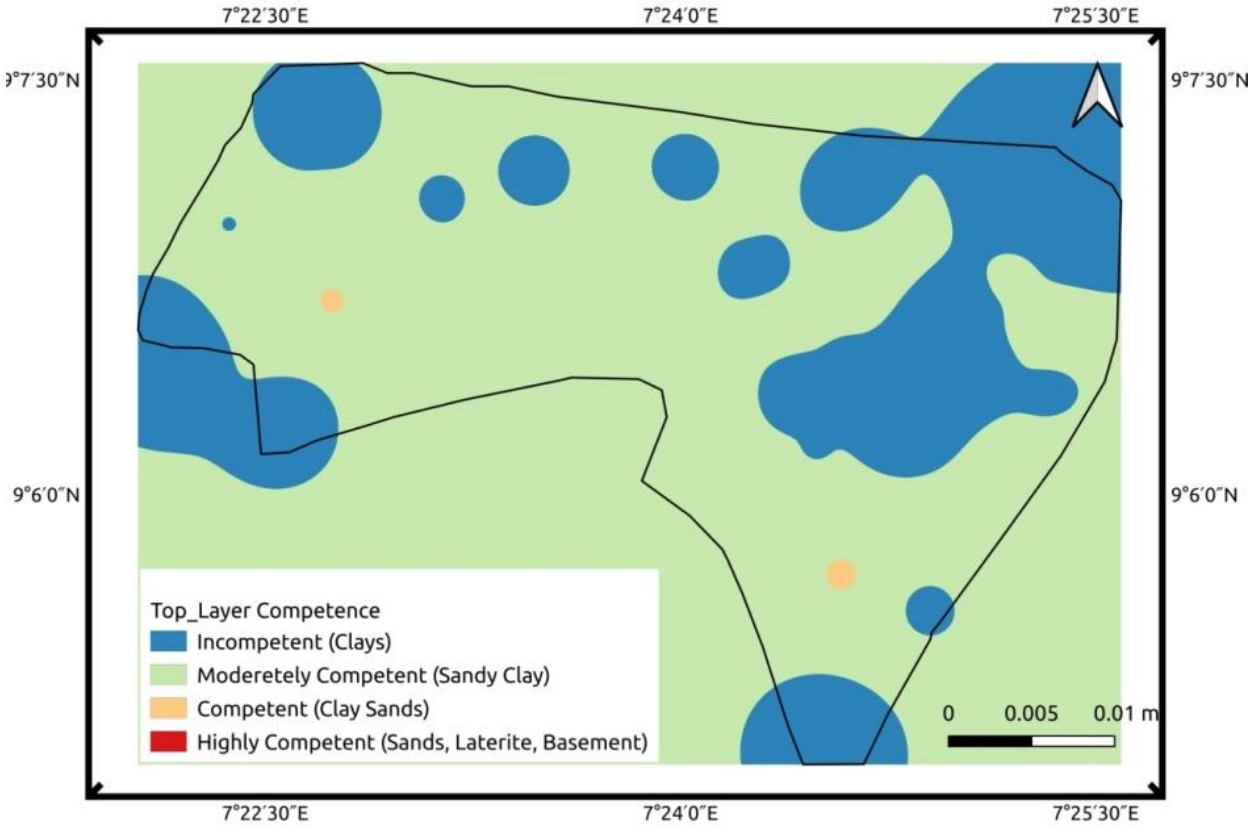

Figure 4: Toplayer competence zonation map of the study area

3.3. AQUIFER PROTECTIVE CAPACITY ASSESSMENT

The protective capacity of the overburden against surface contaminants was evaluated using an integrated approach based on four parameters.

3.3.1. Overburden Thickness

The total overburden thickness, representing the sum of all layers above the fresh basement, ranges from 0.5 m to 16.46 m (Fig. 5), with an average of 4.92 m. About 85% of the area has an overburden thickness less than 10 m, indicating moderately shallow aquifers. Areas with thicker overburden (>10 m), primarily in the central zone, offer better physical protection to the underlying aquifers.

The protective capacity of the study area based on the overburden thickness is presented on Figure 6. According to Ayua et al., (2024), the overburden acts as a barrier to protect the underlying groundwater from contamination. This is intuitively grasped as a thicker overburden can better help prevent contaminants from reaching the groundwater. The study area's eastern and western portions have thin overburden and thus has a very low to low protective capacity (colour code blue to green). Regions with colour code red have the thickest overburden materials and on that basis are adjudged to offer very good protection from superficial contaminants, in accordance with Olatunji-Adeniyi et al (2024), who holds that he thicker the overburden layer, the less susceptible it is to superficial contamination.

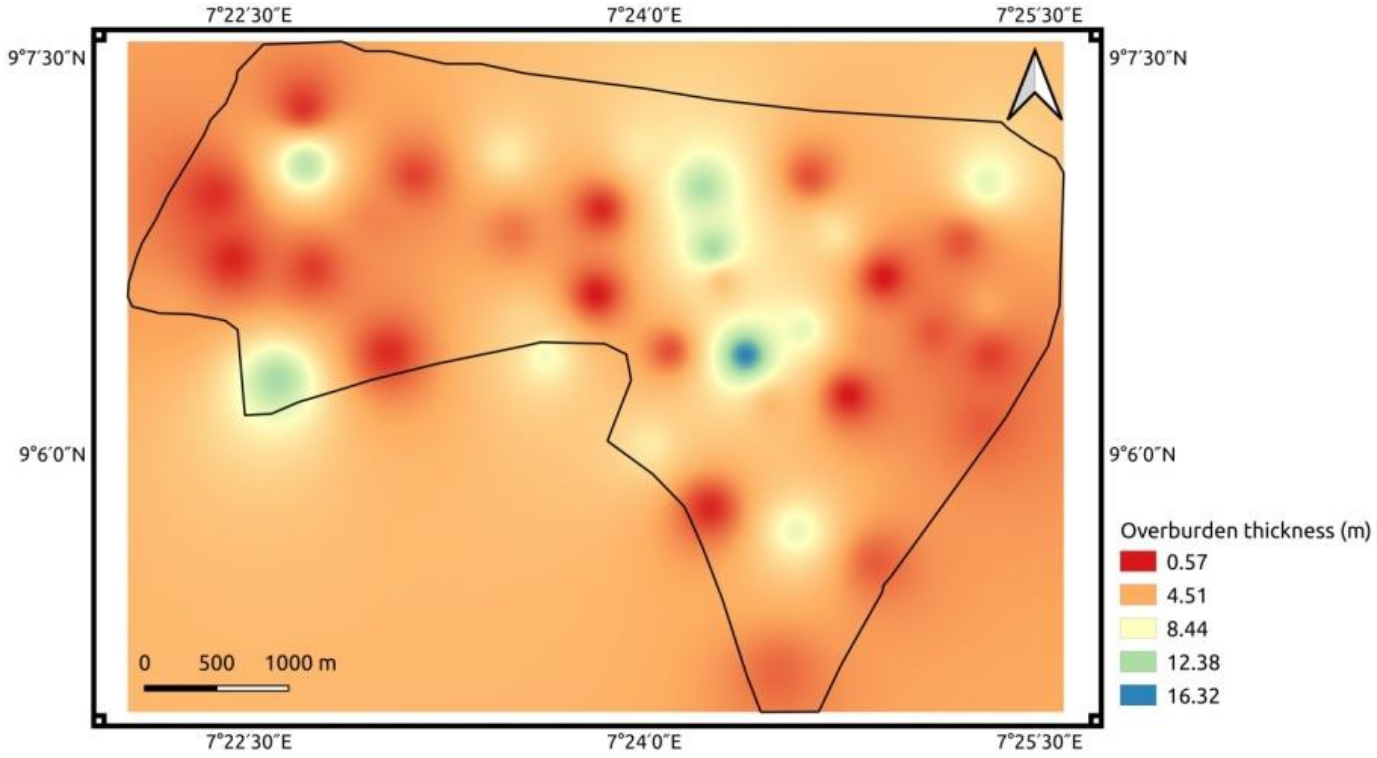

Figure 5: Aquifer Overburden thickness distribution of the study area

Areas with colour code yellow, especially in the north and central portions have moderate aquifer protection capacity on the basis of the overburden thickness. In addition to physical protection, a thicker overburden can also provide better filtration of contaminants, allowing for natural processes to break down or remove pollutants before they reach the aquifer (Ayua et al., 2024; Olatunji-Adeniyi et al., 2024). Conversely, as also argued by Ayua et al., (2024), a thin overburden, except in cases where it is composed of highly impervious materials, may not provide adequate protection for the aquifer, making it more vulnerable to contamination from surface activities such as industrial spills, agricultural runoff, or improper waste disposal. In such cases, pollutants can easily seep through the overburden and contaminate the groundwater, posing a threat to human health and the environment.

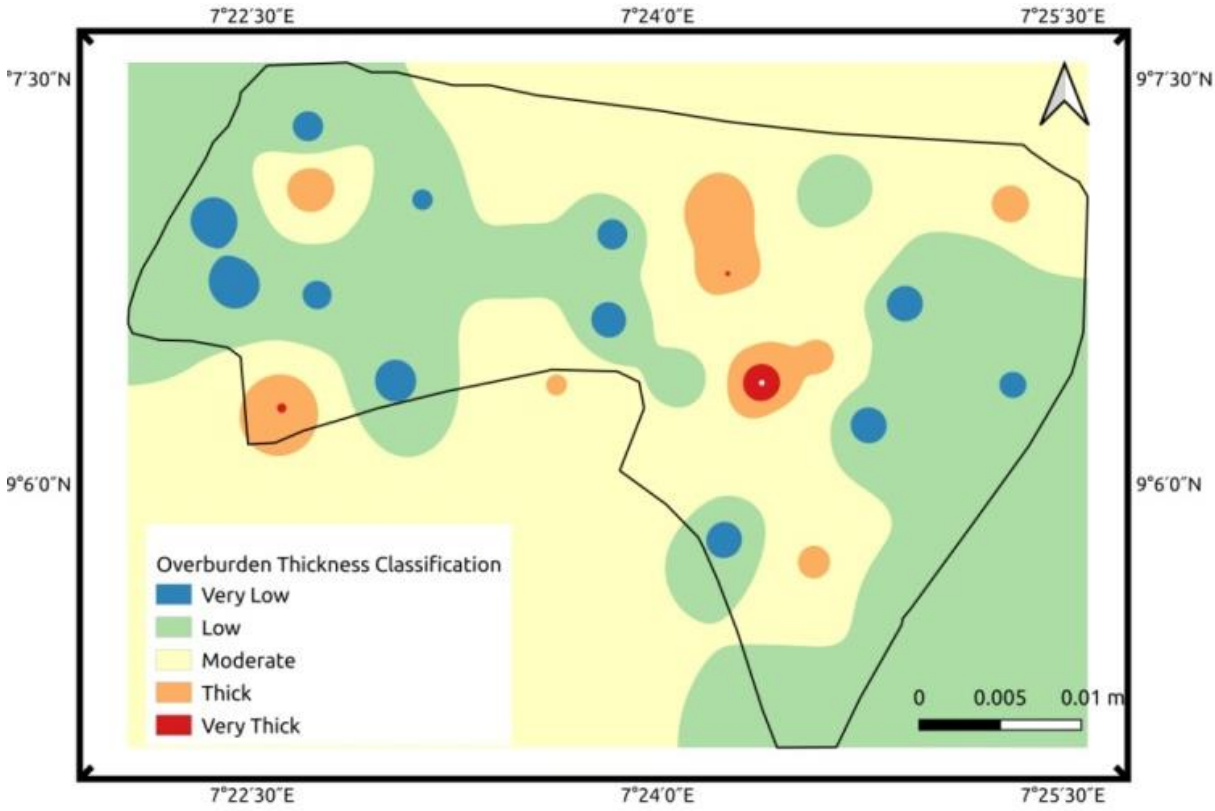

Figure 6: Aquifer Overburden thickness reclassification for overburden protective capacity

3.3.2. Longitudinal Conductance (S)

Ayua et al., (2024), identified the main barrier to contamination of unconfined aquifers, like those in the present research area, to be the existence of underlying clay layers, whose hydraulic characteristics controls the delay between contaminant incursion and influx to the aquifer. These have been shown to be correlated with the longitudinal conductivity or its alternate appellation, integrated Electrical Conductivity.

The longitudinal values obtained in our study area ranges from 0.003 to 3.7 S spanning three orders of magnitude (Fig. 7). The average value for the study area is 0.58 S with a standard deviation of 0.33. While the majority of longitudinal conductivity values are moderately clustered (Mean = 0.58 S, SD = 0.33), the full range of data (0.003 - 3.7 S) indicates significant physical heterogeneity within the study area. This suggests that while a homogeneous model may be a simplifying assumption and may validate our earlier assumption of a homogeneous geological environment, the extreme high-end values (especially in the northeastern portions of the study area) are not captured by this model and likely represent important localized anomalies implying the actual geological environment exhibits considerable variability. The spatial distribution of the longitudinal conductance values (Fig. 4.48) are therefore used to assess heterogeneity rather than global statistics alone.

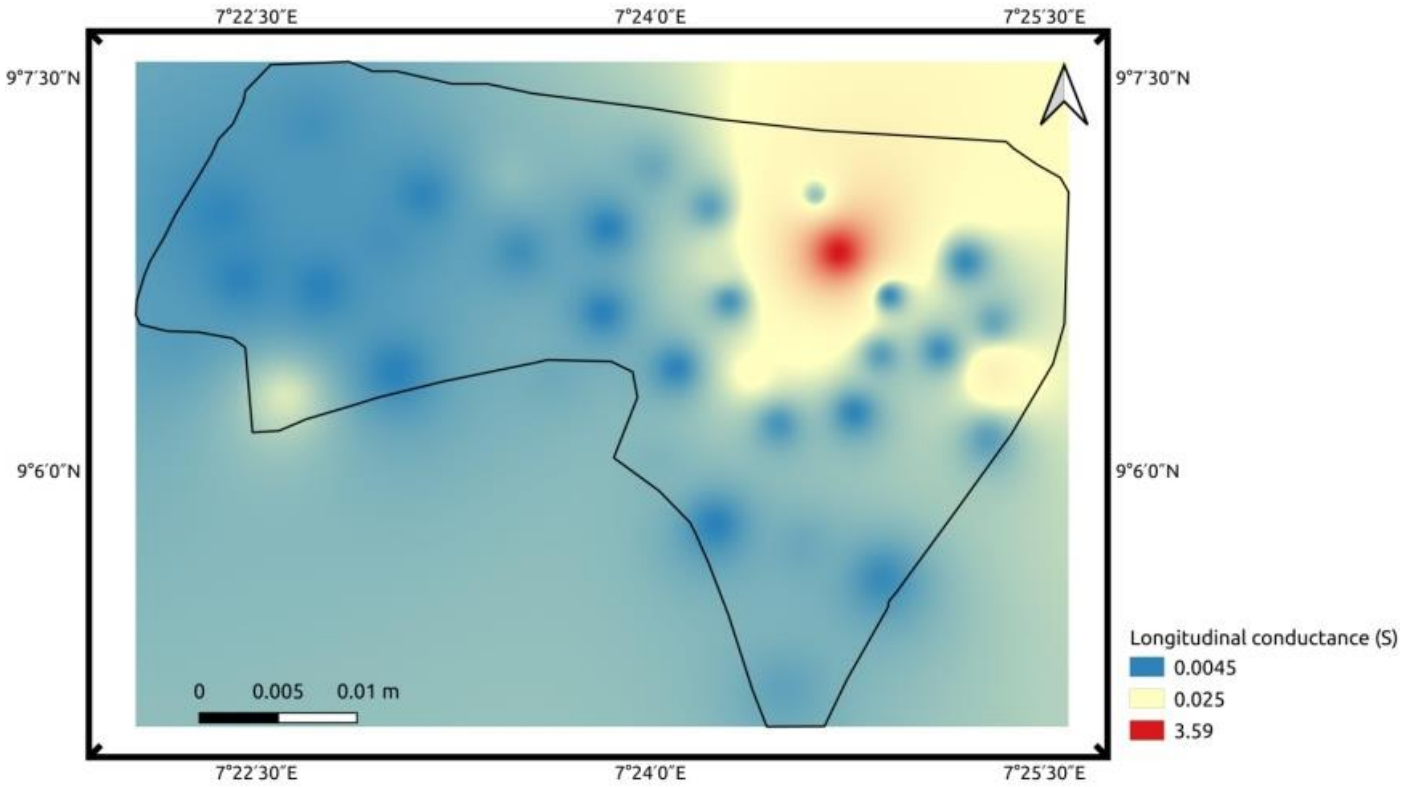

Figure 7: Longitudinal conductance distribution of the study area

Several researches as already discussed in the literature segment have satisfactorily linked the longitudinal conductance (S) of the overburden materials with the level of protection offered to an aquifer since it is a measure of the clay content in a rock material. The longitudinal conductance values were reclassified according to Oladapo et al (2004) and the resulting overburden protective capacity rating is shown in Figure 8.

The study area is classified into four aquifer protective capacity zones, rated from poor to good protective capacity areas (Fig 8). According to Ojo et al. (2015), pervious materials like sand and gravel have low longitudinal conductance values linked to their high resistivity, whereas highly impermeable materials like clay and shale typically have high longitudinal conductance values governed by their low resistivity. The study area however is made up predominantly (about 85%) of overburden materials rated as having poor to weak protective capacity (blue to dark green colour code). The northeastern zone however is composed of high longitudinal conductance materials and thus classified as moderate to good Aquifer protective capacity.

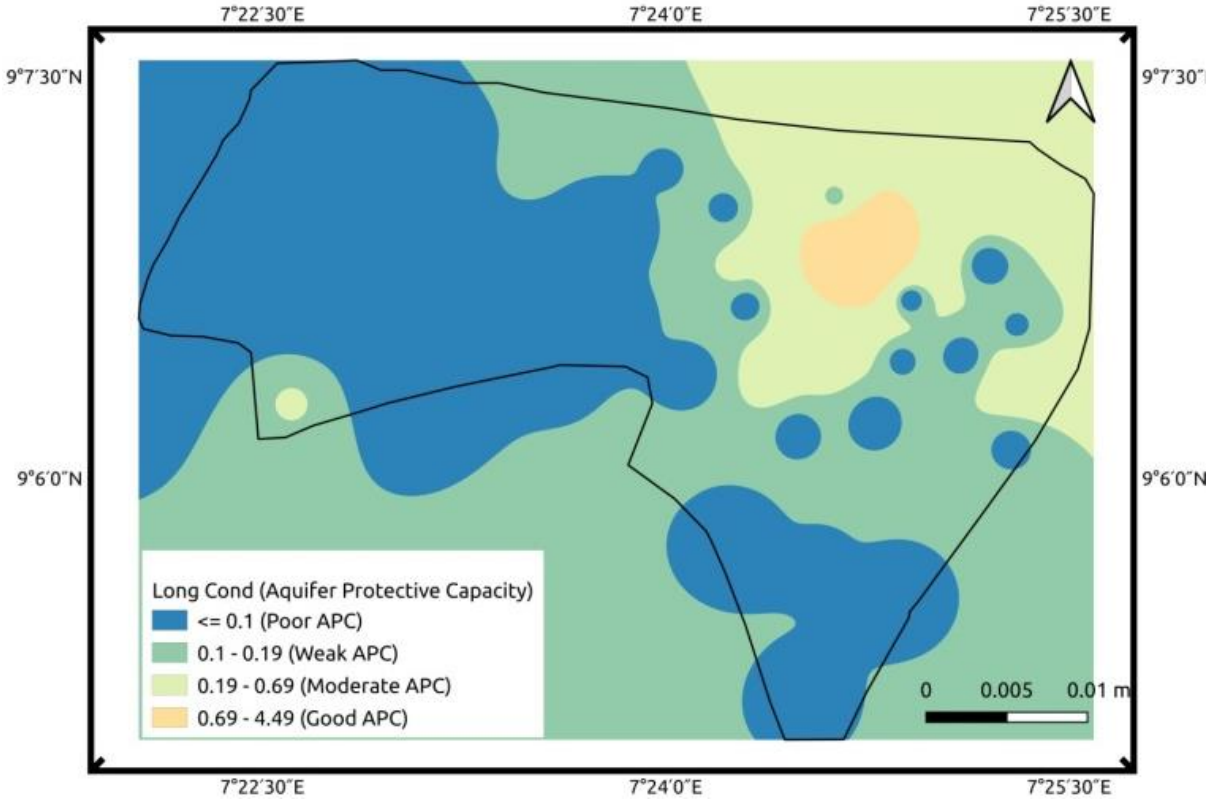

Figure 8: Longitudinal conductance reclassification for aquifer protective capacity

3.3.3. Aquifer Vulnerability Index (AVI)

AVI method was made use of to measure the overburden material's potentiality as a protective covering for aquifers. The AVI technique has been shown (Stempvoort et al. (1993), Obiora & Ibuot (2020), Ayua et al., (2024)) to measures the hydraulic resistance to the vertical fluid flow through the overlying layers, hence implicitly evaluating the covering layers' imperviousness to surficial pollutants (Ayua et al., 2024). The hydraulic resistance Map of the study area and the classified AVI are presented as Figures 9 and 10 respectively.

The hydraulic resistance values across the study area exhibit high variability, ranging from 32.30 to 575.16 (Fig. 9). The significant standard deviation (136.63) and high coefficient of variation (~69%) indicate that the data is not tightly clustered around the mean (197.36). The large gap between the mean and maximum value suggests a right-skewed distribution, where a majority of values are moderate but a few locations exhibit very high resistance (green to blue colour coded areas).

The above statistical profile is inconsistent with a homogeneous geological environment, a conclusion that is at once at variance with the apriori geological knowledge of the study area. However, this statistical profile is understood as likely pointing to localized heterogeneous features within the subsurface. These features could include significant variations in aquifer thickness, the presence of low-permeability zones (e.g., clay layers), or local changes in lithology that create sharp contrasts in hydraulic properties.

Using the AVI technique, the study area is zoned into two classifications of Aquifer vulnerability (Fig. 10) – high vulnerability, moderate/medium vulnerability zones.

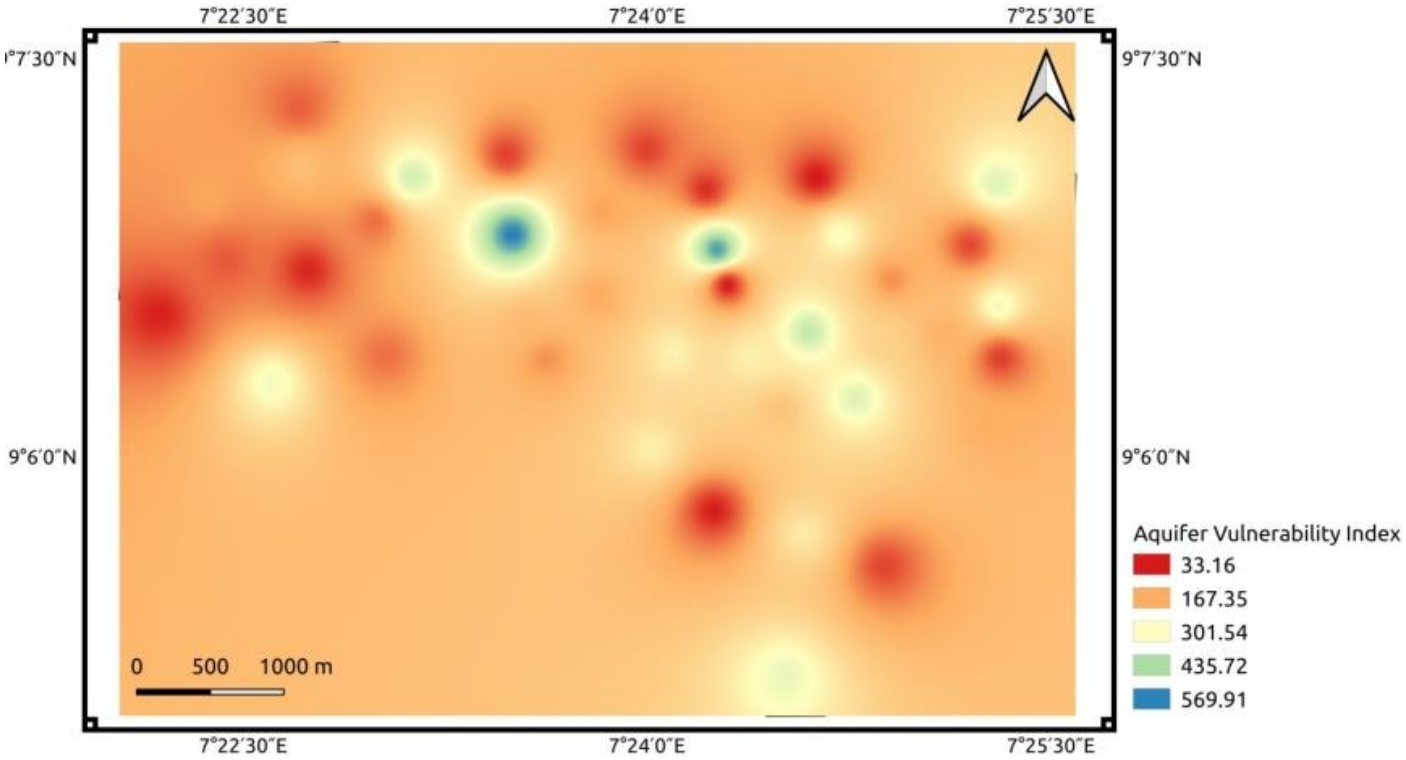

Figure 9: Aquifer Vulnerabilty Index distribution of the study area

Unlike the longitudinal-conductance-based overburden protective capacity zonation (Fig 8), the aquifers in the study area are predominantly classified as having high vulnerability index with medium/moderate vulnerability to pollution (red colour code) in several spatial locations especially in the eastern and central portions of the study area (Fig. 10).

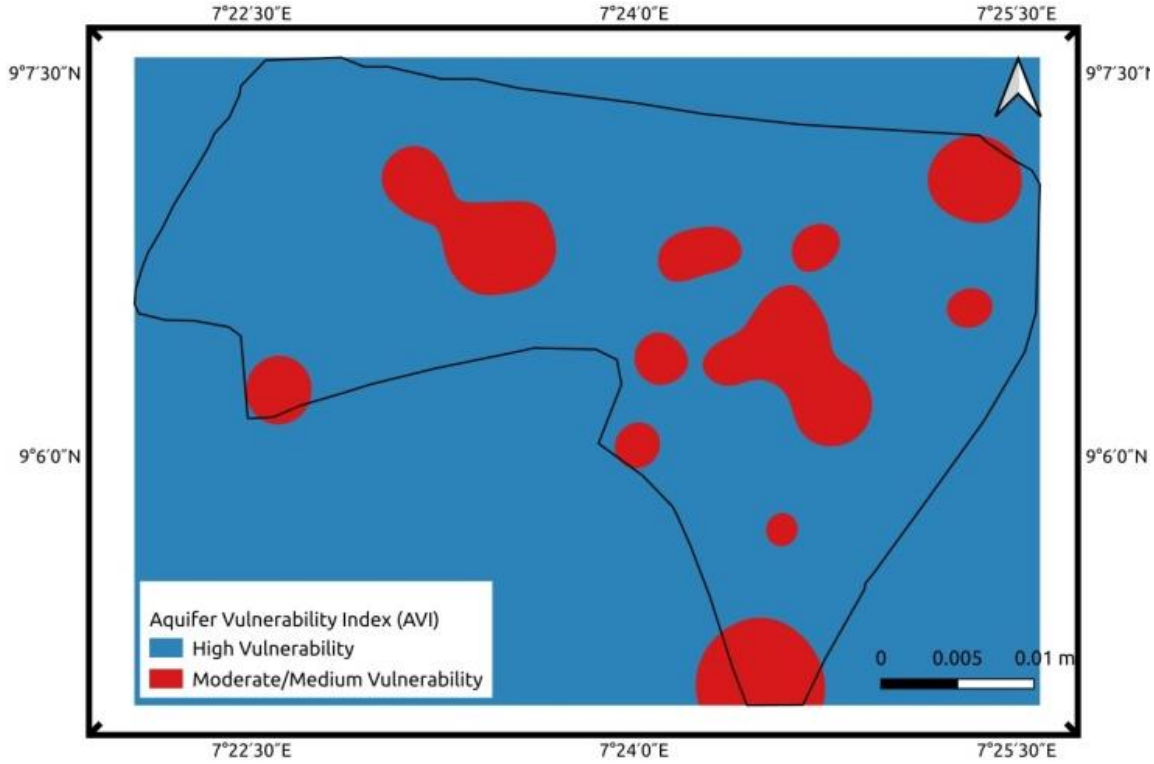

Figure 10: AVI reclassification for aquifer protective capacity

3.3.4. Coefficient of Electrical Anisotropy (λ)

A cursory examinations of both the IEC and AVI results reveal that these indices of measuring APC seem to have been significantly influenced by the overburden thickness. This finding is in line with the studies by Ducci & Sellerino (2013) and Ducci & Sellerino (2022) who reported the tendency for AVI to show higher vulnerability results in superficial aquifers. The reverse seem to be the case in our study area as the thickness of the overburden have seemingly masked the effect of the nature (how clayey it is or not) of the overburden materials. To mitigate the above situation, the coefficient of electrical anisotropy has been computed in order to evaluate the degree of fracture or inhomogeneity within overburden rock materials.

According to Ayua et al. (2024), near-surface characteristics like contrasting degrees of weathering and structural features including faults, fractures, joints, foliations, and beddings may contribute to the creation of effective porosity or secondary porosity (Ogungbemi et al. 2013). These may constitute incipient and preferential pathways for contaminating fluids to seep into aquifers, thus reducing the time lag, and rendering inefficient the natural filtration action of thick overburden beds. The Coefficient of electrical anisotropy distribution within the study area is presented as Figure 11.

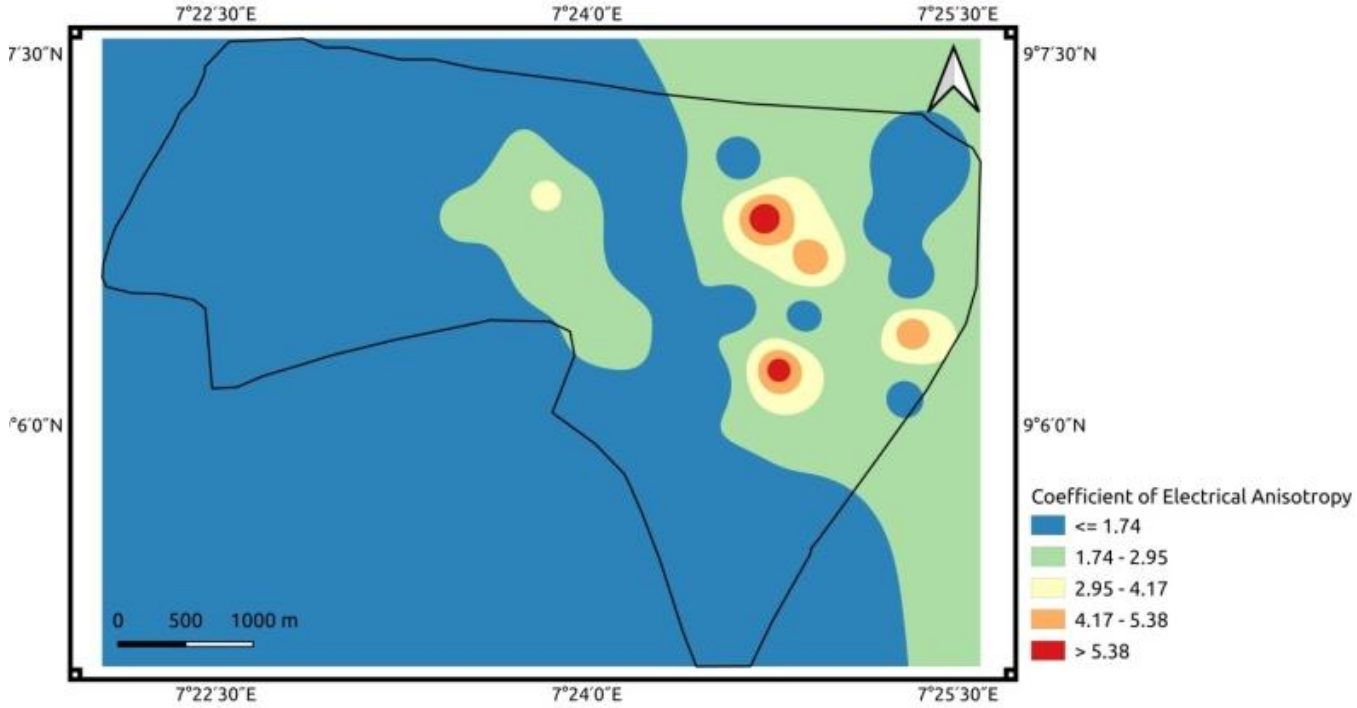

Figure 11: Coefficinet of electrical anisotropy distribution of the study area

From Figure 11, the electrical anisotropy coefficient across the study area exhibits extreme variability (0.5 to 6.6), with a high standard deviation (1.5) and a mean of 1.7.

The dominant anisotropy values falls at about the mean (1.7) or below with values of 1.0 representing perfectly isotropic medium. These results agree with the values obtained for areas underlain by metamorphic rocks in the southwestern part of Nigeria (Olorunfemi *et al.,* 1991), as well as those reported by Ayua et al (2024) in basement complex Lokoja. Values below 1.0 would suggest the medium is more conductive in the vertical direction than the horizontal, which is unusual and can indicate features like vertical fracturing, an occurrence that is important for contamination seepage into aquifers.

The observed standard deviation (1.5) is of comparable magnitude to the mean (1.7), signifying substantial dispersion within the dataset rather than a concentration of values around the central tendency. Furthermore, the proximity of the mean (1.7) to the lower bound (0.5), as opposed to the upper bound (6.6), provides strong evidence of positive skewness. This distributional asymmetry implies that the majority of measurements correspond to moderate, background levels of anisotropy as is clearly seen in Figure 11. A limited number of observations with markedly elevated anisotropy values (approaching 6.6) function as statistical outliers, exerting an upward influence on the mean and inflating the variability. The very high coefficient of variation (~88%) and the right-skewed distribution of the data conclusively demonstrate a heterogeneous subsurface environment. This variability reflects significant spatial changes in the directional electrical properties of the

rocks, likely driven by a complex geological framework featuring a mixture of features such as micro-fractures, and interlayering of materials with strongly contrasting resistivity.

The anisotropy values were then used to evaluate the overburden protective capacity and the results are presented as Figure 12. Since anisotropy values mirror migration pathways and are indicative of secondary porosity, regions of high anisotropy may be indicative of pathways for fluid migration and possible pathways for aquifer contamination, hence the study area was classified into three zones. Low anisotropy areas were classified as having elevated aquifer protection. Zones with medium anisotropy values were classified as having moderate or adequate aquifer protection and regions of high anisotropy values were classified as having elevated risk of aquifer contamination or poor aquifer protection.

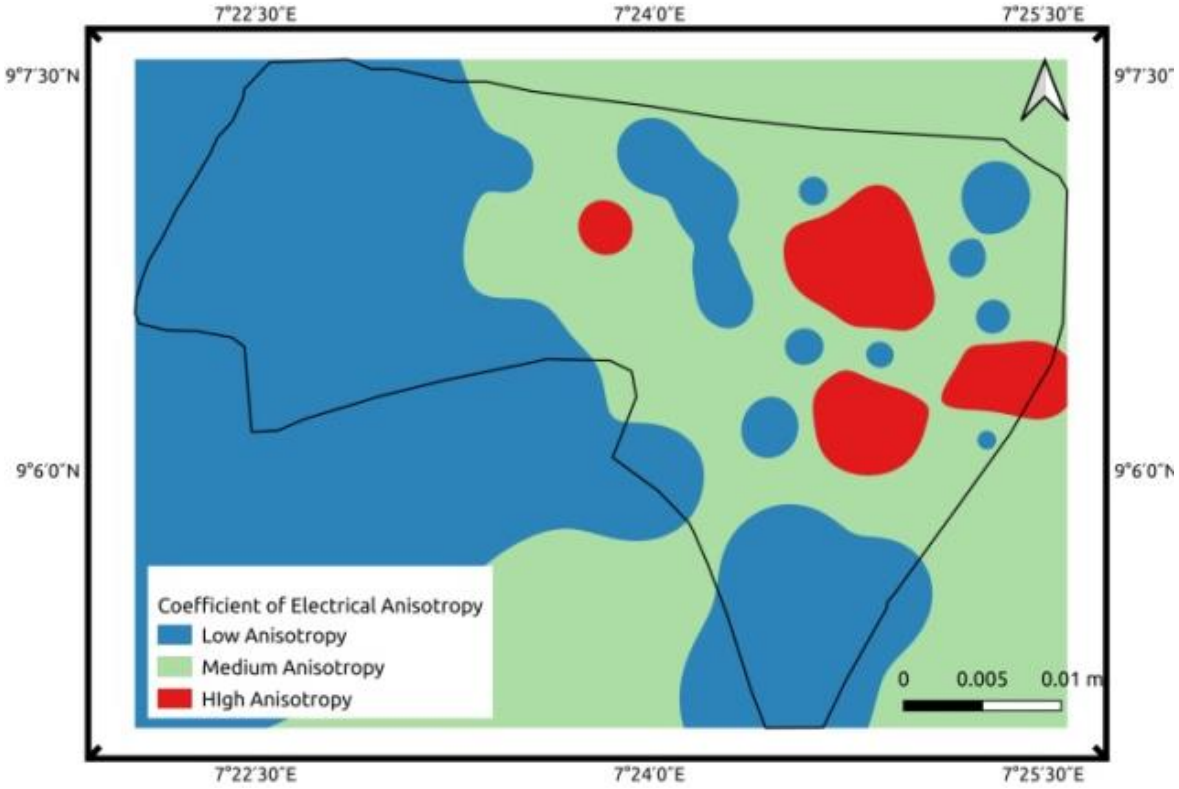

Figure 12: Electrical coefficient of anisotropy reclassification for aquifer protective capacity

3.3.5. Composite Aquifer Protective Capacity Map

The aquifer protective capacity maps generated from the overburden thickness (weight 31%), the IEC (weight 22%), the AVI (weight 22%) and the Coefficient of Electrical Anisotropy (weight 26%) were used as inputs in a weighted Overlay to produce the composite Aquifer Protection Capacity (APC) Map of the study area presented as Figure 13.

The spatial variability of aquifer protective capacity within the study area reveals three distinct hydrogeological zones: poor, moderate, and good protection. The western and eastern flanks exhibit poor aquifer protection, primarily controlled by shallow overburden thickness. These zones are further characterized by low to moderate longitudinal conductance, reflecting a paucity of clayey materials, and elevated anisotropy values, which denote enhanced secondary porosity and the potential for preferential contaminant migration pathways into the underlying aquifer system.

The central sector demonstrates moderate aquifer protection (yellow-coded zone), corresponding to intermediate overburden thickness, moderate clay content inferred from longitudinal conductance, moderate to low anisotropy, and appreciable hydraulic resistance. These factors collectively imply a partially effective but not entirely impermeable protective barrier.

Conversely, a northwest–southeast trending corridor (blue-coded zone) traversing the central portion exhibits the highest degree of aquifer protection. This domain is associated with substantial overburden thickness and enhanced clay accumulation, conditions that synergistically confer high hydraulic resistance. The relatively low anisotropy values in this region further suggest a minimal presence of structural discontinuities such as faults or lineaments, thereby reducing the likelihood of secondary permeability and subsequent contaminant ingress into the aquifer matrix.

Figure 13: composite Aquifer Protection Capacity (APC) Map of the study area presented

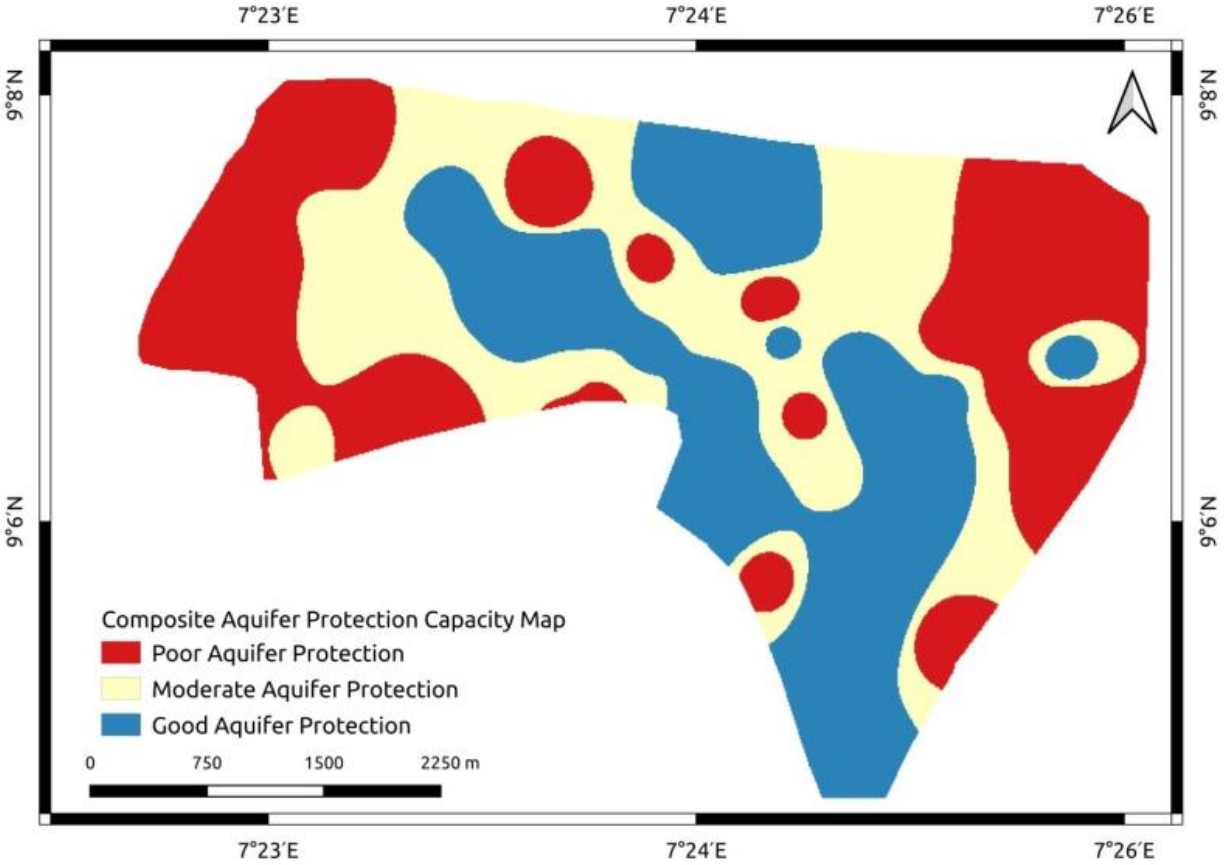

3.4. LABORATORY SOIL ANALYSIS AND GEOTECHNICAL ASSESSMENT

A critical review of the laboratory data reveals a significant inconsistency: samples with very low clay content (e.g., Sample 4 at 1.04%) report exceptionally high Plasticity Index (PI) values (e.g., 67.76). In soil mechanics, a high PI is characteristic of clayey soils, not sandy ones. This suggests a potential error in the determination or reporting of the PI. Therefore, the following discussion prioritizes the grain size distribution data for interpretation.

Table 3: Summary of Laboratory Soil Test Results

Sample	% Sand	% Silt	% Clay	PI	Compaction (kPa)	Strength	Unconfined Strength (kPa)	Compressive
1	55.52	27.20	17.28	55.52	~55		~78	
2	65.52	23.60	10.86	65.52	~65		~65	
3	62.80	25.20	12.00	62.80	~60		~60	
4	67.76	31.20	1.04	67.76	~67		~67	
5	64.80	28.48	6.72	64.80	~64		~64	
6	60.80	27.20	12.00	60.80	~67		~67	

The laboratory results indicate that the soils are predominantly sandy, with sand content ranging from 55.52% to 67.76%. The clay content is generally low (1.04% to 17.28%). This composition implies good drainage characteristics but low cohesion. The unconfined compressive strength (UCS) values, which are critical for foundation design, range from approximately 55 kPa to 78 kPa. These values are very low; for context, typical allowable bearing pressures for shallow foundations in sandy soils often start around 100-150 kPa. The measured strengths suggest that these soils, in their natural state, are suitable only for very light structural loads.

Sample Four, with the highest sand content (67.76%) and a UCS of ~67 kPa, is the most competent among the samples but still requires verification for anything beyond light structures. Sample Six, with a moderate clay content (12%) and a UCS of ~67 kPa, also shows promise for light to moderately loaded structures. The other samples (One, Two, Three, and Five) all have UCS values below or near 65 kPa, indicating a need for soil improvement techniques like stabilization or the use of deep foundations for any significant construction.

4.0 DISCUSSION OF SALIENT FINDINGS

This integrated study successfully characterized the near-surface conditions in Gwarinpa, Abuja, for geotechnical and hydrogeological purposes. The geophysical investigation revealed a relatively homogeneous weathered basement environment, as evidenced by the predominance of H-type VES curves. The aquifer system is predominantly unconfined, hosted within the weathered layer, and generally shallow, with 85% of the aquifers lying within 10 m of the surface.

The dual assessment of soil competency and aquifer protection reveals a clear interplay between geology and land-use suitability. The central parts of the study area, characterized by thicker overburden and lower electrical anisotropy, offer the best natural protection for groundwater resources. In contrast, the western and eastern flanks are more vulnerable to contamination due to thinner overburden and potential fracturing. The geotechnical zonation based on resistivity correlates well with the general understanding of the area, showing a mix of moderately competent and incompetent zones.

The laboratory soil tests provide critical ground-truthing, confirming the sandy nature of the topsoil inferred from the geophysics. However, the very low unconfined compressive strengths measured (55-78 kPa) are a major finding with significant practical implications. They quantitatively confirm that soil stabilization (e.g., with cement, lime, or mechanical compaction) is not just beneficial but essential for supporting standard building foundations in most of the area. The discrepancy between the reported PI and clay content highlights the need for rigorous quality control in laboratory testing and reporting.

5.0 CONCLUSIONS AND RECOMMENDATIONS

This integrated geophysical and geotechnical study successfully delineates the subsurface conditions of the Gwarinpa area, revealing a landscape with distinct opportunities and constraints for sustainable development. The research confirms that the area is underlain by a weathered basement complex, characterized by generally shallow and unconfined aquifers. This geological setting directly influences both the engineering and environmental parameters observed.

From a geotechnical perspective, the sandy topsoil, while offering good drainage, is characterized by a low unconfined compressive strength of merely 55 to 78 kPa. This inherently limits its load-bearing capacity, indicating that without significant intervention, the ground is unsuitable for supporting anything beyond light-weight structures. Consequently, for any substantive development to proceed safely, soil stabilization is not merely an option but a fundamental prerequisite.

Simultaneously, the environmental vulnerability of the area presents a significant concern. The assessment of the aquifer's protective capacity reveals a moderate to poor rating across much of the study area. Particularly vulnerable zones in the western and eastern parts feature a thin and fractured overburden, creating direct pathways for potential contaminants to reach the shallow groundwater. This interplay between geological structure and hydrological risk necessitates a proactive and informed management strategy.

Therefore, the findings of this study compel a series of integrated recommendations. Urban planning authorities must utilize the generated zoning maps to strategically guide future development, directing heavy infrastructure towards the more competent and less vulnerable zones identified. For the construction industry,

the mandate is clear: site-specific geotechnical investigations and the implementation of advanced soil stabilization techniques are essential to mitigate the inherent risks and ensure structural integrity.

To safeguard public health and water resources, environmental protection must be prioritized through the enforcement of land-use regulations in high-vulnerability areas. This would involve restricting high-risk activities, such as unlined waste disposal, which could compromise the already fragile aquifer system. Finally, to refine our understanding and enhance the precision of future development plans, further research employing more dense soil sampling, deeper borehole logging, and advanced 2D/3D geophysical imaging is strongly encouraged. In conclusion, the path to sustainable development in Gwarinpa lies in heeding this scientific evidence, ensuring that growth is built on a foundation of safety, resilience, and environmental stewardship.

COMPETING INTEREST

Authors have declared that they have no known competing or financial interest OR non-financial interests, or personal relationships that could have appeared to influence the work reported in the paper.

REFERENCES

Adeyemo, I., Oluwatimilehin, A. V., & Sanusi, S. O. (2022). Application of TOPSIS and AHP model in subsurface layers competence evaluation: A case study of Ilaramokin, Southwestern Nigeria. https://doi.org/10.21203/rs.3.rs-2373590/v1

Agada, L. E., & Yakubu, M. S. (2022). Evaluation of aquifer protective capacity using electrical resistivity method in Lambata, Kwali Area Council, Abuja. *FUDMA Journal of Science (FJC)*, 6(3), 191–199.

Akintorinwa, O. J., & Abiola, O. (2011). Subsoil evaluation for foundation study using geophysical and geotechnical approaches. *Journal of Emerging Trends in Engineering and Applied Sciences*, 2(5), 858–863.

Alagbe, S. A. (1979). The geology of Jidu – Gidan Anfani – Karumo district of the FCT with emphasis on the relationship of porphyroblastic and non-porphyroblastic rocks (*Unpublished B.Sc. Thesis*). Ahmadu Bello University, Zaria, Nigeria.

Alaminiokuma, G. I., & Chaanda, M. S. (2019). Soil corrosivity profile and aquifer protective capacity in Dukpa, Gwagwalada Area, Crystalline Basement Complex, Nigeria. *IOSR Journal of Applied Geology and Geophysics*, 7(6), 43–51.

Akoachere, R., Yaya, O., Eyong, A., Ayuk, E., & Egbe, E. (2019). Hydrogeology of Abuja FCT-Nigeria: A GIS evaluation. *Open Access Library Journal*, 6, 1–35. https://doi.org/10.4236/oalib.1105649

Ayua, Kuma Joshua. (2025). "Intrinsic Geo-Electric Characterization and Geomorphological Valuation for Groundwater Recharge Potentiality: Implications for Groundwater Sustainability". Journal of Geography, Environment and Earth Science International 29 (6):11-30. https://doi.org/10.9734/jgeesi/2025/v29i6903.

Ayua, K. J., Alimi, G. I., Bamigbaiye, F. F., & Akbar, A. J. (2024). Synthesizing vulnerability indices within a diverse lithological context: Corollaries for groundwater quality assurance and surface layer corrosiveness of Lokoja geomaterials, Nigeria. *Water Practice and Technology*, 19(9), 3744–3762. https://doi.org/10.2166/wpt.2024.201

Ayua, K. J., Uzer, J. M., & Dongel, H. E. (2025). Inherent geoelectric characterization for topsoil integrity analysis in Lokoja using geophysical VES method. *Pakistan Journal of Geology*, 9(2), 96–101. https://doi.org/10.26480/pjg.02.2025.96.101

Bayowa, O., Ogungbesan, G., Aderele, I. O., Alagbe, A. O., Olubosun, A. S., & Olasukanmi, N. (2023). Groundwater potential assessment of shallow aquifers in the basement complex underlain Osogbo metropolis,

Southwest Nigeria, using geo-electric attributes. *Environmental Earth Science.* https://doi.org/10.1007/s12665-023-11509-7

Ducci, D., & Sellerino, M. A. (2013). Vulnerability mapping of groundwater contamination based on 3D lithostratigraphy models of porous aquifers. *Science of the Total Environment*, 447, 315–322. https://doi.org/10.1016/j.scitotenv.2012.12.090

Ducci, D., & Sellerino, M. A. (2022). Modified AVI model for groundwater vulnerability mapping: Case studies in southern Italy. *Water*, 14(2), 248. https://doi.org/10.3390/w14020248

Etuk, M., Viaroli, S., Ogbonnaya, I., & Re, V. (2022). Vulnerability mapping as a tool to foster groundwater protection in areas subject to rapid population expansion: The case study of Abuja Federal Capital Territory, Nigeria. *Journal of Hydrology: Regional Studies*, 42, 101158. https://doi.org/10.1016/j.ejrh.2022.101158

Eze, S. U., & Ayua, K. J. (2025). Monitoring the contamination dynamics and flow pathway of oil spill using 3D–4D ERT in a pollution site. *Environmental Monitoring and Assessment*, 197, 651. https://doi.org/10.1007/s10661-025-14062-x

Idornigie, A. I., & Olorunfemi, M. O. (2006). Electrical resistivity determination of surface layers, subsoil competence, and soil corrosivity at an engineering site location in Akungba Akoko, southwestern Nigeria. *Life Journal of Science*, 8, 22–32. https://doi.org/10.4314/ijs.v8i2.32216

Joshua, A. K., Ilozobhie, A. J., Ikechukwu, E. D., & Agbasi, O. (2023). Scrutinate proclivity of regional aquifer hydraulic parameters: Apriorisms for borehole failures within parts of the middle Benue Trough, Nigeria. *Water Practice and Technology*, 18(12), 3347–3364. https://doi.org/10.2166/wpt.2023.211

Obiora, D. N., & Ibuot, J. C. (2020). Geophysical assessment of aquifer vulnerability and management: A case study of University of Nigeria, Nsukka, Enugu State. *Applied Water Science*, 10, 29. https://doi.org/10.1007/s13201-019-1113-7

Ofomola, M. O., Iserhien-Emekeme, R. E., Okocha, F. O., & Adeoye, T. O. (2018). Evaluation of subsoil competence for foundation studies at site III of the Delta State University, Nigeria. *Journal of Geophysics and Engineering*, 15, 638–657.

Ojo, S., Olorunfemi, J. O., Akintorinwa, M. J., Bayode, O. S., Omosuyi, G. O., & Akinluyi, F. O. (2015). Subsoil competence characterization of the Akure metropolis, southwest Nigeria. *Journal of Geography, Environment and Earth Science International*, 3(1), 1–14.

Oladapo, M. I., Mohammed, M. Z., Adeoye, O. O., & Adetola, O. O. (2004). Geoelectric investigation of the Ondo State Housing Corporation Estate Ijapo Akure, southwestern Nigeria. *Journal of Mining and Geology*, 40(1), 41–48.

Olatunji-Adeniyi, O., Ayua, K. J., & Osisanya, O. W. (2024). Assessment of aquifer protective capacity of Orire Estate in Akure, Ondo State, Nigeria. *Journal of Applied Sciences and Environmental Management*, 28(10B Supplementary), 3439–3452.

Olorunfemi, M. O., Olarewaju, V. O., & Alade, O. (1991). On the electrical anisotropy and groundwater yield in a basement complex area of Southwestern Nigeria. *Journal of African Earth Sciences*, 12(3), 467–472.

Ogungbemi, O. S., Badmus, G. O., Ayeni, O. G., & Ologe, O. L. (2013). Geoelectric investigation of aquifer vulnerability within Afe Babalola University, Ado-Ekiti, Southwestern Nigeria. *IOSR Journal of Applied Geology and Geophysics*, 1(5), 1–7.

Rajapakse, R. (2016). Site investigation and soil conditions. In *Pile Design and Construction Rules of Thumb* (2nd ed., pp. 1–30). Butterworth-Heinemann.

Samuel, A. O., Mohammed, A. B., Onunuju, O. C., & Mathew, S. J. (2022). Geological investigation of soil conditions for foundation study of Kukwaba, Abuja. *ASEANA Journal of Science and Education*, 2(1), 1–8.

Stempvoort, D. V., Ewert, L., & Wassenaar, L. (1993). Aquifer vulnerability index: A GIS-compatible method for groundwater vulnerability mapping. *Canadian Water Resources Journal*, 18(1), 25–37.

Vander Velpen, B. P. A. (2004). *WinRESIST version 1.0: Resistivity sounding interpretation software.* M.Sc. Research Project, ITC, Delft, Netherlands.